Journal of Glaucoma Publish Ahead of Print
DOI:10.1097/IJG.0000000000002096

Novel Tomographical Bleb Classification Following ab-interno Implantation of Gel-Stent Using Anterior Segment Optical Coherence Tomography.

Authors:

Somar M. Hasan, MD[1], Theresa Theilig, MD[1], Melih Tarhan, MD[1], Menelaos Papadimitriou, MD[1], Jan Darius Unterlauft, MD[2], Daniel Meller, MD[1]

Affiliations:

[1] Department of Ophthalmology, Jena University Hospital, Germany

[2] Department of Ophthalmology, Bern University Hospital, Switzerland

Corresponding author:
Somar M. Hasan, MD
Address: Department of Ophthalmology, Jena University Hospital, Am Klinikum 1, 07747, Jena
Fax: +4936419329702
Telephone: +4936419329733
E-mail: Somar.Hasan@med.uni-jena.de

Disclosure of funding:
none

Running title:
Tomographical Classification of Filtering Bleb Following ab-interno Implantation of Gel-Stent

Précis:

A novel qualitative tomographical classification for bleb following implantation of XEN-Gel-Stent using ab-interno approach is presented. Association of anatomical patterns to IOP and success rates illustrates that AS-OCT can be useful tool in clinical guidance.

Abstract

Purpose:

To present a novel classification of bleb resulting from ab-interno implantation of XEN-Gel-Stent and report association of tomographical patterns with intraocular pressure (IOP) and success rates (SR).

Materials and Methods:

A cross-sectional one-armed study of patients receiving XEN-Gel-Stent. Tomographical changes in the bleb area were studied using swept-source optical coherence tomography in an early (day 29 to 90 post-surgery) and late (starting from day 91 post-surgery) phase. Frequency of patterns and their association with IOP and SR (defined as IOP<18 mmHg without medications) were studied

Results:

111 examinations of 49 blebs (49 patients) were included. 3 tomographical patterns at conjunctival, 4 at tenons capsule and 2 at episcleral level were characterized. Most frequent conjunctival pattern was subepithelial spaces (56.3% and 53.2%in the early and late phase, respectively) and associated with lower IOP (13.0±6.0mmHg) and higher SR (89%) but only in the early phase compared to other conjunctival patterns ($p<0.05$). At tenons capsule level, the hyporeflective pattern was most frequent (50% and 51.9% in early and late phase) followed by the cavernous pattern. Both patterns associated with lower IOP and higher SR compared to hyperreflective or loss of tenon changes ($p<0.005$). Most blebs showed no episcleral lake (87.5% and 89.9% in early and late phase). No difference of IOP and SR was noted compared to those showing an episcleral lake.

Conclusion:

A practical and clinically relevant novel classification system is proposed to tomographically

describe and classify blebs following implantation of XEN-Gel-Stent. Certain patterns were associated with lower IOP and higher SR.

Keywords:

Bleb classification, Anterior segment optical coherence tomography, XEN Gel Stent, Glaucoma surgery.

Introduction:

The subconjunctival space is the most effective outflow pathway in glaucoma surgery for reducing intraocular pressure (IOP). Various surgical techniques utilize it as in trabeculectomy (TE), non-penetrating filtration surgeries and glaucoma drainage devices. The resulting bleb and its assessment are vital for surgical success [1]. Many classification systems have been presented to evaluate the bleb morphology and correlate it to the resulting IOP and need for further interventions or determining follow-up intervals[2, 3].

The use of anterior segment optical coherence tomography (AS-OCT) to evaluate bleb after filtering glaucoma surgery has dramatically increased in the last years as it offers an objective and reproducible assessment tool [4-7] compared to sole subjective appraisal using biomicroscopy or photography. AS-OCT may even offer a better prognostic evaluation of the bleb compared with clinical examination [8, 9]. Different patterns of changes at the conjunctival and subconjunctival level were described and multiple qualitative and quantitative evaluation systems have been developed before [4, 7, 10-12].

As the XEN-Gel-Stent (XEN) was introduced as -till now- the only ab-interno procedure for filtering surgery targeting the subconjunctival space, many surgeons adapted already available grading systems for blebs after TE and applied these systems to assess the morphology of the resulting bleb after XEN. However, this practice may have different obstacles: firstly, the ab-interno approach and abolition of conjunctival and tenon dissection are very likely to result in a different bleb morphology compared with an ab-externo approach. Also, the outer orifice of the XEN is located about 5 mm posterior to the limbus resulting in significantly more posterior filtration and therefore to a more posteriorly located bleb compared to TE. In addition, the length and lumen diameter of the XEN ensure more regular and uniform outflow compared to TE which might also affect the morphology of the resulting bleb. The application of Mitomycin C (MMC) by injection into a space not previously dissected and leaving it in

situ may also have an effect. All this raise significant concerns about the suitability of available bleb grading systems which are primarily developed for TE whether using biomicroscopy or AS-OCT based systems.

The main aim of this study was to utilize AS-OCT techniques to examine the tomographical morphology of blebs resulting from an ab-interno implantation of XEN, to classify tomographical patterns found and study their correlation to IOP along with creating a practical grading system to help describe and classify these blebs in daily practice.

Materials and Methods:

This was an observational cross-sectional single armed study performed between March 2020 and December 2021. Included were only one eye of each patient with primary open-angle or pseudoexfoliation glaucoma undergoing implantation of XEN-Stent (Allergan Inc., CA, USA, an Abbvie company, IL, USA) with application of subconjunctival MMC. Inclusion and exclusion criteria are listed in Table-1. Patients with pseudoexfoliative glaucoma were included as these have shown comparable results to patients with primary open angle glaucoma in previous studies [13]. All patients appeared to post-operative follow-up between March 2020 and December 2021 received an AS-OCT. The same bleb was allowed to be included more than once if bleb classification changed in the following examinations, if not, only first examination was included and following ones were not evaluated.

Included were only examinations starting from the 5^{th} post-operative week to avoid the fast-changing morphology of blebs during the first 4 weeks. Excluded were eyes which underwent any form of intra- or post-operative surgical conjunctival manipulation on the bleb, including needling or open bleb revision. Preoperative data were collected at the time of surgical indication including age, sex, visual acuity (using Snellen chart), IOP (using Goldmann applanation tonometry), number of glaucoma medications, history of previous eye surgeries and concomitant ocular diseases. Post-operatively, following data were collected: date of

surgery, date of follow-up, IOP and number of glaucoma medications at the time of follow-up along with intra- and post-operative complications. AS-OCT was performed on every post-operative visit using a standardized protocol and resulting images were analyzed as described below.

Surgical Technique:

The periocular skin and the conjunctiva were disinfected with povidone iodine (10 and 5% solution, respectively). Intraoperative gonioscopy was performed to check the anterior chamber angle and to choose the best location for stent implantation in the superior nasal quadrant. Conjunctiva was marked 3 mm from limbus. A subconjunctival injection of 0.1 ml of MMC (0.2mg/ml) was delivered about 5 mm from limbus. The resulting cyst was massaged posteriorly and anteriorly, avoiding to reach the limbus. A 2.0mm inferotemporal clear corneal incision was made along with a nasal paracentesis. The anterior chamber was filled with cohesive viscoelastic and the XEN-Gel-Stent was injected superior to the trabecular meshwork into the subconjunctival space aiming to the 3 mm mark on the conjunctiva. The location and distance of the stent to cornea and iris were checked by gonioscopy. The stent's distal segment was checked for mobility using a spatula. Using this approach, a subconjunctival placement of the stent was likely achieved in most cases. However, an exact localization of the outer segment is not possible as the conjunctiva was not opened.

Preoperatively all glaucoma medications were paused for 4 weeks and patients were put on Dexamethasone eyedrops 5x daily (Dexapos COMOD 1.0mg/ml eye drops, Ursapharm, Saarbrücken, Germany) and oral Acetazolamid 250 mg (Glauopax® 250 mg tablets, Omni-Vision, Puchheim, Germany) whose dose was titrated according to IOP measurements. Postoperative regimen included Ofloxacin eye drops 5x daily for 1 month (Floxal® 3mg/ml eye drops, Bausch&Lomb, Laval, Canada) und Dexmethasone eyedrops (Dexapos COMOD

1.0mg/ml eye drops, Ursapharm, Saarbrücken, Germany) q2h in the first week and then 5x daily starting from day 8. Dexamethasone was reduced by 1 drop per day every 4 weeks. According to this regimen, patients received Dexamethason eye drops over 5 months postoperatively.

Anterior Segment OCT:

We used a high resolution swept-source AS-OCT (ANTERION®, Heidelberg Engineering GmbH, Heidelberg, Germany). Examinations were performed using a standard protocol. The patient was asked to look downwards and temporally to expose the bleb. The upper lid was gently lifted up using a cotton swab avoiding exerting any pressure on the globe. A 7 mm wide rectangular box with 45 scans was centered on the stent with active eye-tracking being turned off. Scans were positioned in two directions: the first with the scans oriented parallel to the stent (mostly radial to limbus) and the second with the scans oriented perpendicular to the stent (mostly tangential to limbus) as shown in Figure-1. Care was taken to include the distal opening of the stent in the scans. This resulted in 90 scans of each bleb at each follow-up examination.

Morphological Classification of Blebs:

At each follow-up 90 scans / bleb were analyzed. After reviewing all scans and defining the anatomical structures (conjunctiva, tenons capsule, episcleral lake and the sclera), we observed different patterns of changes at the level of each anatomical structure. A representative image of each distinct pattern was chosen. Using these illustrative images, two independent observers (SMH and TT) classified each bleb. Both were masked to patients' clinical data. In case of discrepancy, the case was discussed until agreement was achieved.

Main outcomes were classification of each bleb and the frequency of each morphological pattern. Mean IOP and surgical success were compared between different patterns at the same

anatomical level. Surgical success was defined as having an IOP of less than 18mmHg without any medication[14]. We consider this to be a realistic target of this micro invasive surgical technique which primarily targets patients with mild to moderate disease and aims to get patients free of medications.

To examine changes of bleb morphology over time, outcomes were studied at two different time points: during the early post-operative phase, defined as day 29 to day 90 after surgery and the late post-operative phase starting from day 91 post-surgery. The role of preoperative medications in bleb morphology and success rates (SR) were also studied. Effect of each medication class on the frequency of morphological patterns or on SR was analyzed.

Statistical analysis was performed using SPSS 22.0 (Armonk, NY: IBM Corp. IBM Corp). Data were tested for normal variance and results were presented as mean±standard deviation (±SD). Dependent and Independent t-sample tests were used to compare means when applicable, otherwise Wilcoxon or Mann-Whitney U tests were performed. Agreement between observers was tested using Kappa measure of agreement. Association between IOP lowering medications, patterns and surgical success were studied using Pearson Chi-Square test.

All procedures performed involving human participants were conducted in accordance with the ethical standards of the institutional research committee and with the Declaration of Helsinki

Results:

Included were 111 examinations of 49 eyes (49 patients), 9990 scans were performed and analyzed. The demographic data are presented in Table-2.

Mean IOP dropped from 20.1±4.8 pre-operatively to 15.7±5.1 mmHg ($p<0.001$) postoperatively corresponding to a mean decrease of 4.5±6.6mmHg and 22.4%. Mean number of glaucoma medications reduced from 2.9±1.0 to 0.2±0.6 ($p<0.001$), a reduction of 93.1%.

Following assessment of all captured scans, we were able to classify morphological changes in the bleb area according to their anatomic location into 9 patterns. Representative images are shown in Figure-2. At the conjunctival level, we observed three distinct patterns: 1. no changes of the observed conjunctiva (C0) 2. small conjunctival cysts or vesicles (C1) 3. Presence of wide subepithelial spaces lying between conjunctiva and tenons capsule (C2). Observed changes of the conjunctiva were best seen in the tangential AS-OCT scans. At the level of tenons capsule we were able to observe four well defined morphological patterns. While in the first one no tenon changes were seen (T0), hyperreflective changes over the whole bleb area were observed in the second pattern (T1) compared with presence of low reflective areas of tenon in the third pattern (T2). The fourth pattern comprised cavernous changes in form of hollow cavities inside tenons capsule (T3). At the episcleral level, we observed two different patterns: the absence of a visible episcleral lake (ES0) or the presence of an episcleral fluid filled space or cleft (ES1). Episcleral patterns were also best seen in the tangential scans.

Each bleb was classified using this tomographical grading system by addition of the conjunctival, tenonal and episcleral patterns to each other. Mean IOP± standard deviation for each pattern were calculated resulting in the following classification shown in Table-3. As example: a bleb showing subconjunctival spaces (C2) and hyporeflective changes of tenons capsule (T2) with no visible episcleral lake (ES0) was classified as C2T2ES0.

The agreement between the two observers was 0.4 for conjunctival patterns, 0.6 for patterns found in tenons capsule and 0.79 for patterns at the episcleral level (Kappa measure of agreement, $p<0.001$ for all).

Frequency of morphological patterns over each post-operative period is presented in Figure-3

At the conjunctival level, subepithelial spaces (C2) was the most frequent pattern over all follow-up intervals comprising 56.3% in the early phase and 53.2% in the late phase. This decrease was accompanied by increased frequency of epithelial cysts (C1, 28.1% to 34.2% in the early and late phase). The frequency of absence of changes (C0) at the conjunctival level reduced over the follow-up time (15.6%, 12.7%) in the early and late phase, respectively.

At the level of tenons capsule, the most frequent pattern found was hyporeflective changes (T2) with relatively stable proportion of 50.0% and 51.9% in the early and late phase, respectively. On the other hand, the proportion of cavernous changes (T3) increased from 18.8% in the early phase to 32.9% in the late phase. This was accompanied by a decrease in cases where no changes (T0) were noticed (early and late phase: 21.9% and 10.1%, respectively). The proportion of hyperreflective changes (T1) decreased from 9.4%to 5.1% in the early and late phase, respectively.

The episcleral lake was absent (ES0) in the majority of cases (87.5%, 89.9% in the early and late phase, respectively).

Studying Associations of Different Patterns with IOP and SR:

Early Post-Operative Phase (mean time post-surgery: 47.4±19.1 days, N=32)

The mean±SD of IOP and number of glaucoma medications along with SR in the early post-operative phase according to tomographical patterns are shown in Table-4. Box-Plots of IOP in different patterns including significant p-values for the early post-operative phase are shown in Figure-4

The presence of subepithelial spaces (C2) was associated with higher surgical SR compared to its absence (p=0.041). At the tenon level, SR in cases with hyporeflective (T2) or cavernous changes (T3) were significantly higher than in other cases (91% compared to 40%,

respectively, p=0.001). At the level of episclera, SR did not show differences of statistical significance between both groups (p=0.23).

Late Post-Operative Phase (mean time post-surgery = 342.5±249.9 days, N=79):

The mean±SD of IOP and number of glaucoma medications along with SR in the late post-operative phase are shown in Table-5. Box-Plots of IOP in different patterns including significant p-values for the late post-operative phase are shown in Figure-5

At the conjunctival level in the late post-operative phase, we did not observe statistically significant differences regarding SR between different patterns (p>0.05). At the level of tenons capsule, hyporeflective (T2) or cavernous tenonal changes (T3) showed significantly higher SR compared to their absence (81% VS 25%, respectively, p<0.001). No difference of SR was also observed at the episcleral level between the two patterns (p=0.12).

Studying the role of preoperative medications in bleb morphology and success rates:

Association of each class of medications to the frequency of each morphological pattern and SR was studied. Patterns T2 and T3 were grouped together as these seem to be two morphologies with similar function.

The use of beta blockers preoperatively associated with increased frequency of patterns C1 and C2 (p=0.026, Chi-Square test). No other associations of betablockers with other patterns were observed. Use of carbonic anhydrase inhibitors or prostaglandins preoperatively did not associate with any changed frequency of morphological patterns (p>0.05 for all). The use of alpha 2-agonists preoperatively associated with a significant decreased frequency of pattern T1 (p=0.002), an increased frequency of patterns T2 and T3 (p=0.002) and a decreased frequency of pattern ES1 (p=0.013). No association of any of the medications with the SR was found (p>0.05 for all).

Discussion:

The XEN-Gel-Stent is a unique device utilizing the subconjunctival outflow pathway through an ab-interno approach. This results in a conjunctival bleb whose evaluation is critical in leading post-operative follow-up and thereby surgical success. Multiple studies examined bleb morphology using biomicroscopy, stereophotography as well as AS-OCT and multiple grading systems exist to classify blebs following TE. Many clinicians and authors adapted these for the examination and classification of blebs following implantation of XEN. However, the ab-interno approach along with its posterior location and abolishment of surgical dissection of conjunctiva and tenons capsule, injection of MMC without washing it out and the expected uniform flow of aqueous humor through the stent make the bleb morphology after XEN differ significantly from that after TE [15], and thus, requires modification of used evaluation systems .

Very few studies describe the morphology of blebs following XEN using AS-OCT. Sacchi et al. examined it and compared it to that after TE and observed lower bleb height and bleb wall reflectivity along with higher number of epithelial cysts after XEN compared with TE [15]. Teus et al. observed similar findings in addition to much smaller cystic cavities found after XEN compared to those after TE [16]. Both evaluated quantitative parameters and compared them between blebs following XEN and TE.

There are many obstacles associated with the quantitative assessment of bleb morphology using AS-OCT. Measurements of certain parameters such as bleb height, bleb wall thickness or reflectivity, number and size of epithelial cysts were performed in most studies only at one to three predefined sections [8, 15-18]. However, these parameters, according to our observation in 9990 scans, differ significantly across the same bleb so that a measurement at one predefined scan cannot be sufficient (e.g., Bleb height at a predefined scan might not correspond to the highest point of the bleb or even be representative for the overall height of

one single bleb). In addition, quantitative assessment of different parameters requires special software which is not supplied by most providers and thus only possible using image editing, done most likely manually. Also, measuring same parameters with different machines is likely to result in different outcomes making results less applicable in daily practice. Many of these obstacles might be overcome using two main strategies: 1. increasing the number of performed scans and thus evaluating a larger area of the bleb, optimally capturing the whole bleb and 2. depending on qualitative rather than quantitative assessment, as this naturally comprises a description of a whole image compared with measuring predefined parameters at predefined scans which might lead to under- or overestimation of certain parameters. Using the latter strategy, Wen et al. graded blebs after TE using AS-OCT based on the whole bleb morphology at 2 predefined scans and found a significant correlation with a number of Moorfields Bleb Grading System variables[7]. A classification of morphological changes according to different anatomical levels was not performed.

In our study we performed 90 scans of each bleb, 45 oriented tangentially and 45 oriented radially to the limbus centered on the implant. Bleb classification was performed after evaluating each of these. This gives an overall view of the bleb and lessens the over- or under-estimation of single AS-OCT scans. It also combines description of various patterns at each level allowing for a more consistent description of the whole bleb morphology. This should make the assessment using AS-OCT more similar to what clinicians have always done using biomicroscopy or photography at the slit lamp using known grading systems, still with the advantage of much higher magnification, more objectivity and ability to emphasize deeper layers, not visible during clinical examination.

In this study, we characterized morphologic patterns seen in 111 examinations of 49 blebs and sorted them according to the anatomical layer which resulted in three patterns at the conjunctival level, four at the level of tenons capsule and two at the episcleral level. A

grading system generated using these patterns describes the whole changes of each bleb and is well reproducible. Agreement between two independent observers was good.

In the early post-operative phase (day 29 to 90 post-surgery), most frequent pattern observed at the conjunctival level was the subepithelial spaces (C2). Its frequency however decreased minimally during the late post-operative period (starting from day91) and accompanied by an increased frequency of epithelial cysts (C1). The proportion of eyes with no conjunctival changes (C0) decreased minimally. Eyes with subepithelial spaces in the early phase had significantly lower mean IOPs compared to other patterns and showed higher SR. This difference disappeared during the late post-operative period as all conjunctival patterns showed comparable IOP levels and SR.

The presence of conjunctival cysts seen by biomicroscopy was associated with better bleb function after TE in different grading systems[1, 2]. Subepithelial spaces (or subepithelial separation) were already described in AS-OCT scans following TE and XEN [17, 19]. Lenzhofer et al. reported an association between presence of subconjunctival tissue separation with lower mean IOPs during the course of 12 months after XEN implantation[17]. This was the case in our study only during the early phase but not thereafter. This discrepancy might have different explanations: in their study, Lenzhofer et al. performed 3 scans of each bleb and reported a subconjunctival separation rate of 29-32% in the first 3 months which dropped to 16-22% after that. The proportion of subepithelial spaces in our study was obviously higher and ranged between 56.3% in the first 3 months and 53.2% after that, as we evaluated 90 scans of each bleb and had a higher chance to catch these spaces in the same bleb. Secondly, in their study, Lenzhofer et al. did not exclude eyes which underwent needling or open conjunctival revision, so that changes resulting from these surgical manipulations might have affected bleb morphology and generated such a difference to our study.

At the tenons level, the most frequent pattern observed was hyporeflective changes (T2) with a frequency of 50% and 51.9% in the early and late phase, respectively. The cavernous pattern (T3) was seen in only 18.8% of cases in the early phase. However, this proportion increased to 32.9% in the late phase. An Explanation for this increase might be the tissue remodeling process of the bleb during the first months following surgery, where frequency of blebs with no changes reduced.

Different authors used different models to describe and quantify changes in the subconjunctival area following TE and XEN. Frequently measured was the bleb wall thickness and bleb cavity height following TE [8]. Qualitatively, the reflectivity of the bleb wall and the presence or absence of episcleral lake were also frequently used [11]. In many cases, we were not able to demarcate the bleb wall exactly, especially in cases with present hyporeflective changes (majority of cases) at the tenons level (Figure-6).

These blebs also did not show the classically described fluid accumulation used to measure the bleb cavity height as seen following TE. Even when these were seen as in the cavernous pattern, we had difficulties defining the exact borders of this cavity as most blebs with a present cavernous pattern showed a serous cavity inside a bed of spongy multilayered tissue of tenon capsule (Figure-7).

At the end, we found that classifying blebs depending on bleb wall thickness / reflectivity or on height of bleb cavity was not suitable for most blebs developing after implantation of a XEN in an ab-interno approach.

During assessment of OCT-scans, we noticed that increased hyporeflectivity (T2) at the tenons capsule was associated with ‘clefting’ of layers and sometimes beginning of development of cavernous changes (T3). Both patterns (T2 and T3) were associated with significantly lower IOP values and higher SR compared to other tenonal patterns. Additionally, there was no difference between the two patterns at any time point regarding

resulting IOP or SR. This gives the impression that we are dealing with two morphologies with similar function.

The episcleral lake was absent in the majority of our cases at all time points (ES0, 87.5% and 89.9% in the early and late phase, respectively). Although blebs showing an episcleral lake (ES1) had low IOP and very high SR (100% in the early and late phase), the number of these blebs was too low (4 and 6 in the early and late phase, respectively), to show a difference of statistical significance when compared to blebs without visible episcleral lakes. The presence of this space has been considered a positive sign for a functioning bleb after TE [11]. However, the ab-interno approach and loss of surgical dissection of this space seem to be responsible for its absence in the majority of our cases. When using an ab-externo approach for XEN-Gel-Stent implantation, almost all functioning blebs showed an episcleral lake [18]. Our results support the theory that the episcleral lake can only be established through the surgical dissection of tenons capsule from the sclera which is one of the crucial steps utilized during ab-externo techniques. The presence of this space in a minority of cases can be explained by the deeper implantation of the XEN at the episcleral level. However, the depth of XEN positioning during implantation cannot always be easily defined and controlled.

Our data show that the most relevant tomographical changes regarding IOP and SR appear to happen at the level of the tenons capsule over both follow-up phases. Changes of the conjunctiva, especially the subepithelial spaces (C2) appear to be relevant only in the early postoperative phase and to lose their significance in the late phase. The presence or loss of conjunctival changes of any type did not associate with significant differences of IOP and SR in the late post-operative phase. The rarity of a visible episcleral lake (ES1), most likely due to the ab-interno approach, makes it difficult to assess its relevance to IOP and SR, although a tendency toward lower IOP and higher SR was observed among these blebs.

When studying the effect of preoperative IOP lowering medications, the use of alpha 2 agonists was associated with increased frequency of the patterns T2 and T3 along with a

decreased frequency of the patterns T1 and ES1. The exact mechanism of this effect is not clear. Alpha 2 agonists are highly selective agents for the alpha 2 receptors compared with alpha 1 agonists, still they do affect the alpha 1 receptors and results in conjunctival vasoconstriction[20]. As the patterns T2 and T3 correlate with increased accumulation of aqueous humor at the tenon level compared with other tenon patterns, the vasoconstrictive effect of the alpha 2 agonistis might be responsible for a reduced uptake capacity of conjunctival vessels which results in increased accumulation of aqueous humor and increased frequency of the two morphological patterns T2 and T3 and a reduced frequency of the pattern T1. This possible explanation needs to be verified in larger studies as such an effect was seen in spite of pausing preoperative medications 4 weeks before surgery.

Our Study has several limitations: we included only blebs which received XEN without any kind of other manipulation on the conjunctiva, including needling or open conjunctival revision which are frequently needed after XEN (in up to 45% of cases[21-23]) and included blebs starting from the 5th post-operative week. This restricts our findings to this group of patients. Although it might be interesting to study bleb morphology during the first 4 weeks as many patients do fail in this time period, the high variability and fast changing bleb morphology as well as the significant difference in this morphology compared with that of following postoperative phase make this study very challenging, especially when trying to create such a standardized classification system. Also, our study had a cross-sectional single-armed design, studying differences to other surgical ab-externo techniques (e.g., TE, Preserflo-Microshunt etc.) was not possible. Furthermore, the number of certain patterns was too low to show statistical significance as in the presence of an episcleral lake, so that studying these parameters in larger groups is warranted. Because of the cross-sectional design, we were not able to make any statements regarding the prognostic value of the presented grading system. In addition, 90 scans for each bleb were performed, the most posterior scan was about 7mm from limbus. More posteriorly located changes were not

visible. These changes could affect the classification of a more posteriorly located bleb. Along with the qualitative classification, an automated quantification of epithelial cysts or subepithelial spaces, cystic or cavernous tenon changes might add useful information and support this classification system. However, this type of quantification was not available on the platform we worked with and needs additional specialized software.

On the other hand, this is the first study to our knowledge which presents a novel qualitative classification of blebs following filtering surgery using an ab-interno approach based on AS-OCT findings while using a high number of scans for each bleb with a large cohort of patients and long follow-up period. The presented classification is well reproducible and easy to adapt and showed a good association of certain parameters with resulting post-operative IOP and SR, which gives this system not only a descriptive importance but also a clinical relevance.

References

1. Picht, G. and F. Grehn, [Development of the filtering bleb after trabeculectomy. Classification, histopathology, wound healing process]. Ophthalmologe, 1998. 95(5): p. W380-7.
2. Cantor, L.B., et al., Morphologic classification of filtering blebs after glaucoma filtration surgery: the Indiana Bleb Appearance Grading Scale. J Glaucoma, 2003. 12(3): p. 266-71.
3. Wells, A.P., et al., A pilot study of a system for grading of drainage blebs after glaucoma surgery. J Glaucoma, 2004. 13(6): p. 454-60.
4. Leung, C.K., et al., Analysis of bleb morphology after trabeculectomy with Visante anterior segment optical coherence tomography. Br J Ophthalmol, 2007. 91(3): p. 340-4.
5. Kudsieh, B., et al., Updates on the utility of anterior segment optical coherence tomography in the assessment of filtration blebs after glaucoma surgery. Acta Ophthalmol, 2021.
6. Savini, G., M. Zanini, and P. Barboni, Filtering blebs imaging by optical coherence tomography. Clin Exp Ophthalmol, 2005. 33(5): p. 483-9.
7. Wen, J.C., S.S. Stinnett, and S. Asrani, Comparison of Anterior Segment Optical Coherence Tomography Bleb Grading, Moorfields Bleb Grading System, and Intraocular Pressure After Trabeculectomy. J Glaucoma, 2017. 26(5): p. 403-408.
8. Waibel, S., et al., Bleb Morphology After Mitomycin-C Augmented Trabeculectomy: Comparison Between Clinical Evaluation and Anterior Segment Optical Coherence Tomography. J Glaucoma, 2019. 28(5): p. 447-451.
9. Kokubun, T., et al., Anterior-Segment Optical Coherence Tomography for Predicting Postoperative Outcomes After Trabeculectomy. Curr Eye Res, 2018. 43(6): p. 762-770.
10. Khamar, M.B., et al., Morphology of functioning trabeculectomy blebs using anterior segment optical coherence tomography. Indian J Ophthalmol, 2014. 62(6): p. 711-4.
11. Tominaga, A., et al., The assessment of the filtering bleb function with anterior segment optical coherence tomography. J Glaucoma, 2010. 19(8): p. 551-5.
12. Hirooka, K., et al., Stratus optical coherence tomography study of filtering blebs after primary trabeculectomy with a fornix-based conjunctival flap. Acta Ophthalmol, 2010. 88(1): p. 60-4.
13. Gillmann, K., et al., XEN Gel Stent in Pseudoexfoliative Glaucoma: 2-Year Results of a Prospective Evaluation. J Glaucoma, 2019. 28(8): p. 676-684.
14. Fea, A.M., et al., Evaluation of Bleb Morphology and Reduction in IOP and Glaucoma Medication following Implantation of a Novel Gel Stent. J Ophthalmol, 2017. 2017: p. 9364910.
15. Sacchi, M., et al., Structural imaging of conjunctival filtering blebs in XEN gel implantation and trabeculectomy: a confocal and anterior segment optical coherence tomography study. Graefes Arch Clin Exp Ophthalmol, 2020. 258(8): p. 1763-1770.
16. Teus, M.A., et al., Optical coherence tomography analysis of filtering blebs after long-term, functioning trabeculectomy and XEN(R) stent implant. Graefes Arch Clin Exp Ophthalmol, 2019. 257(5): p. 1005-1011.
17. Lenzhofer, M., et al., Longitudinal bleb morphology in anterior segment OCT after minimally invasive transscleral ab interno Glaucoma Gel Microstent implantation. Acta Ophthalmol, 2019. 97(2): p. e231-e237.
18. Dangda, S., et al., Open Conjunctival Approach for Sub-Tenon's Xen Gel Stent Placement and Bleb Morphology by Anterior Segment Optical Coherence Tomography. J Glaucoma, 2021. 30(11): p. 988-995.

19. Nakano, N., et al., Early trabeculectomy bleb walls on anterior-segment optical coherence tomography. Graefes Arch Clin Exp Ophthalmol, 2010. 248(8): p. 1173-82.
20. Greenfield, D.S., J.M. Liebmann, and R. Ritch, Brimonidine: a new alpha2-adrenoreceptor agonist for glaucoma treatment. J Glaucoma, 1997. 6(4): p. 250-8.
21. Mansouri, K., et al., Two-Year Outcomes of XEN Gel Stent Surgery in Patients with Open-Angle Glaucoma. Ophthalmol Glaucoma, 2019. 2(5): p. 309-318.
22. Reitsamer, H., et al., Two-year results of a multicenter study of the ab interno gelatin implant in medically uncontrolled primary open-angle glaucoma. Graefes Arch Clin Exp Ophthalmol, 2019. 257(5): p. 983-996.
23. Reitsamer, H., et al., Three-year effectiveness and safety of the XEN gel stent as a solo procedure or in combination with phacoemulsification in open-angle glaucoma: a multicentre study. Acta Ophthalmol, 2021.

Legends of Figures:

FIGURE-1 An example of the standard protocol used to examine the bleb area: A one of 45 scans performed radial to limbus. B one of 45 scans performed tangential to limbus, insets: scanned areas shown inside the green rectangles.

Green arrowheads: Epithelial cysts. Blue arrowheads: Subepithelial spaces. White asterisk: Hyporeflective area of tenons capsule. C: Conjunctiva. T: Tenons capsule. S: Sclera. X: XEN-Gel-Stent. White dotted line: Interface between conjunctiva and tenons capsule. Yellow dotted line: Interface between tenons capsule and sclera.

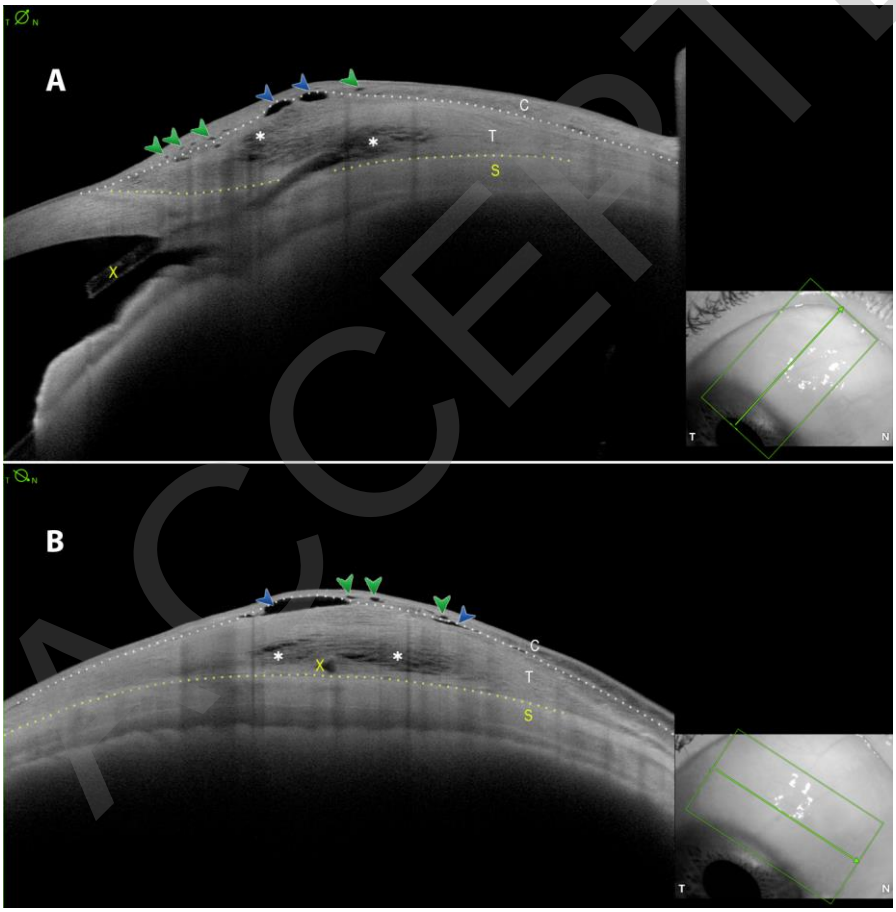

FIGURE-2: Representative images of different patterns found in AS-OCT scans at the three anatomical levels: (C) at the conjunctiva, (T) at the tenons level and (ES) at the episcleral level:

C0: tangential scan of bleb with no conjunctival changes

C1: tangential scan of bleb with epithelial cysts

C2: tangential scan of bleb with subepithelial spaces

T0: radial scan of bleb with no visible changes of tenons capsule

T1: radial scan of bleb with hyperreflective changes of tenons capsule

T2: radial scan of bleb with hyporeflective changes of tenons capsule

T3: radial scan of bleb with cavernous changes of tenons capsule

ES0: tangential scan of bleb with no episcleral lake

ES1: tangential scan of bleb with visible episcleral lake

Green arrowheads: Epithelial cysts. Blue arrowheads: Subepithelial spaces. White asterisk: Hyporeflective area of tenons capsule. Doppel white asterisk: Cavernous space, Yellow asterisk: Subepithelial space. C: Conjunctiva. T: Tenons capsule. S: Sclera. X: XEN-Gel-Stent.

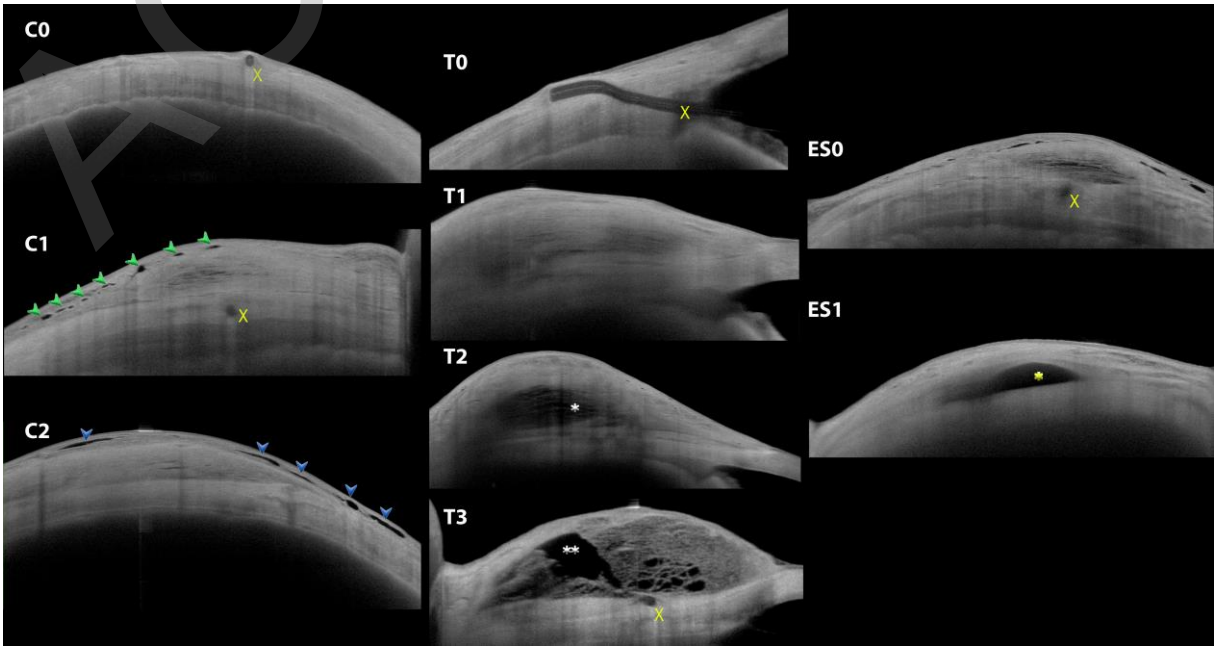

FIGURE-3 Frequency of tomographical changes during early and late phase:

at the conjunctival level: C2 (subepithelial spaces) was the most common pattern followed by C1 (epithelial cysts) in the early and late phase. At the tenon level: T2 (hyporeflective changes) was the most frequent pattern. At the episcleral level: ES0 (no episcleral lake) was the most common pattern with very few blebs showing an ES1 pattern (visible episcleral lake).

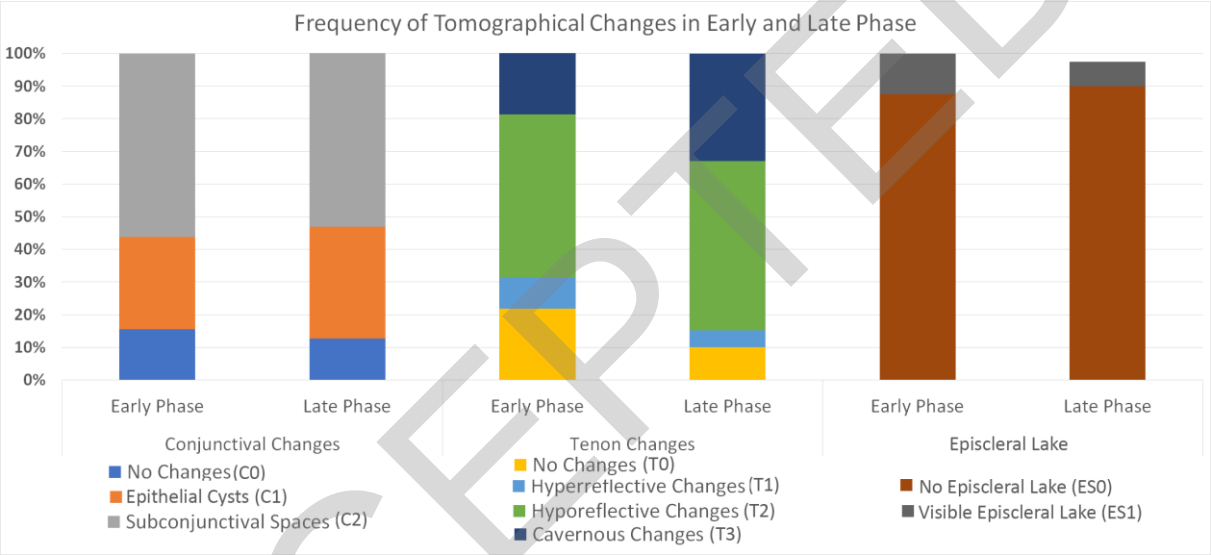

FIGURE-4 Boxplots of IOP in early post-operative phase at different anatomical layers. C2 pattern was associated with lower IOP compared to C0. T2 and T3 were associated with lower IOP when compared to T0. No difference of IOP was observed between patterns ES0 and ES1.

* p<0,05, ** p≤0.001

Abbreviation: IOP intraocular pressure

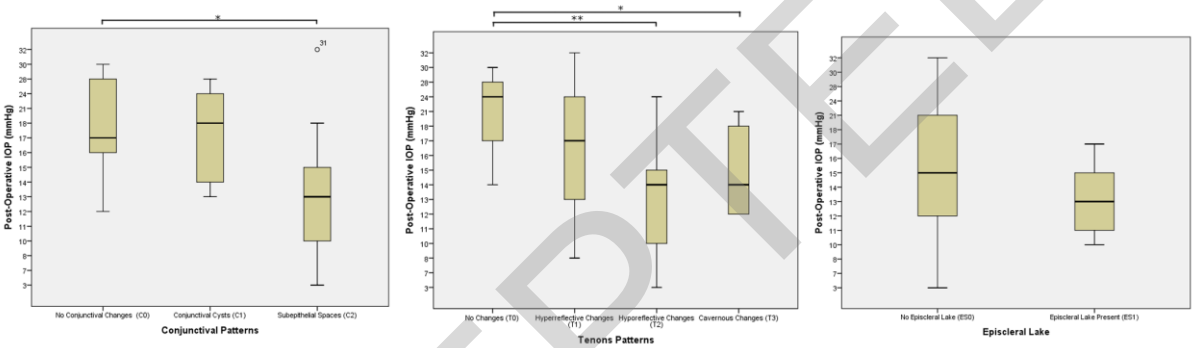

FIGURE-5 Boxplots of IOP in late post-operative phase at different anatomical layers: no differences between C0, C1 and C2 patterns regarding IOP were noticed in the late post-operative phase. T2 and T3 patterns showed significant lower IOP when compared to T0 or T1. No difference of IOP between ES0 and ES1 was also observed in this phase.

** p≤0.002

Abbreviation: IOP intraocular pressure

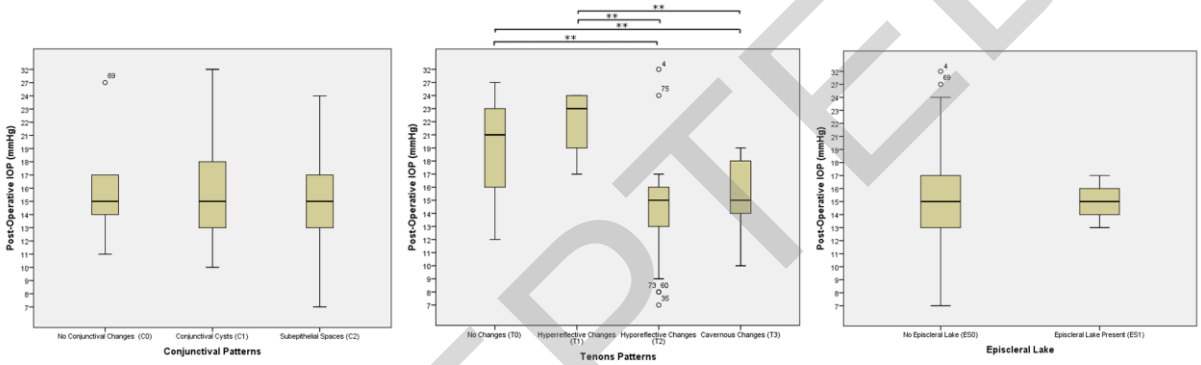

FIGURE-6 Example of a bleb classified as C2T2ES0 (most common pattern in this study). The absence of a typical serous cavity which is a characteristic manifestation of the hyporeflective form (T2), makes the measurement of bleb wall thickness not possible.

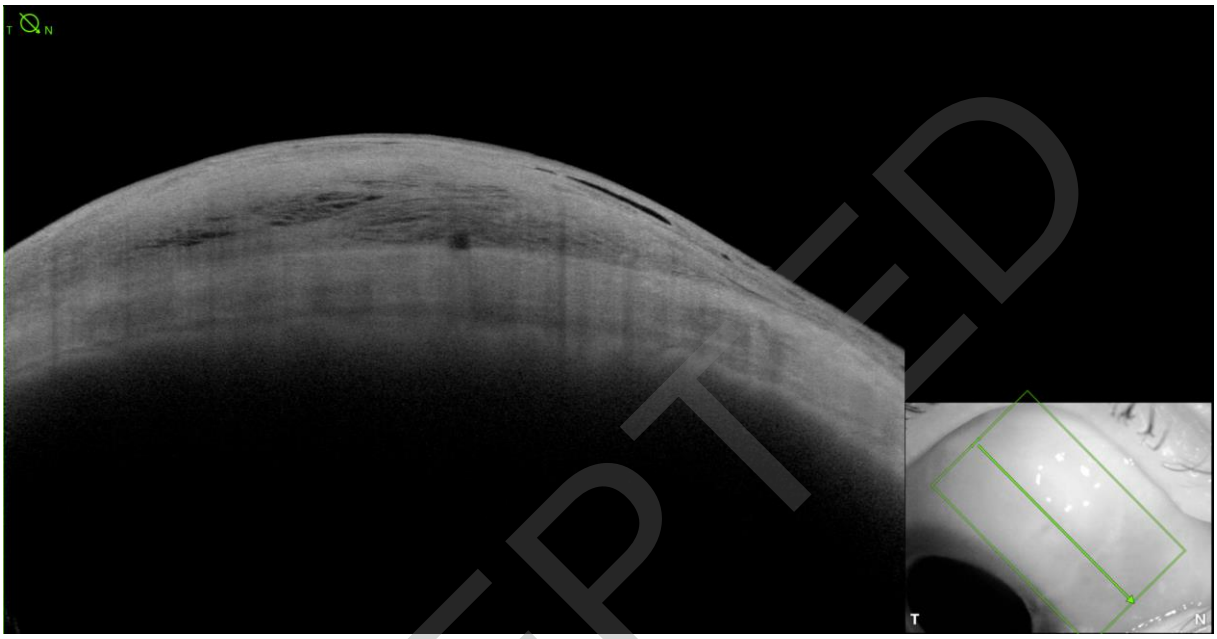

FIGURE-7 Even in cases where a serous cavity was observed (C1T3ES0 in this example), it was not always possible to define the borders of this cavity as it was found inside a bed of spongy multilayered hyporeflective tissue of tenons capsule.

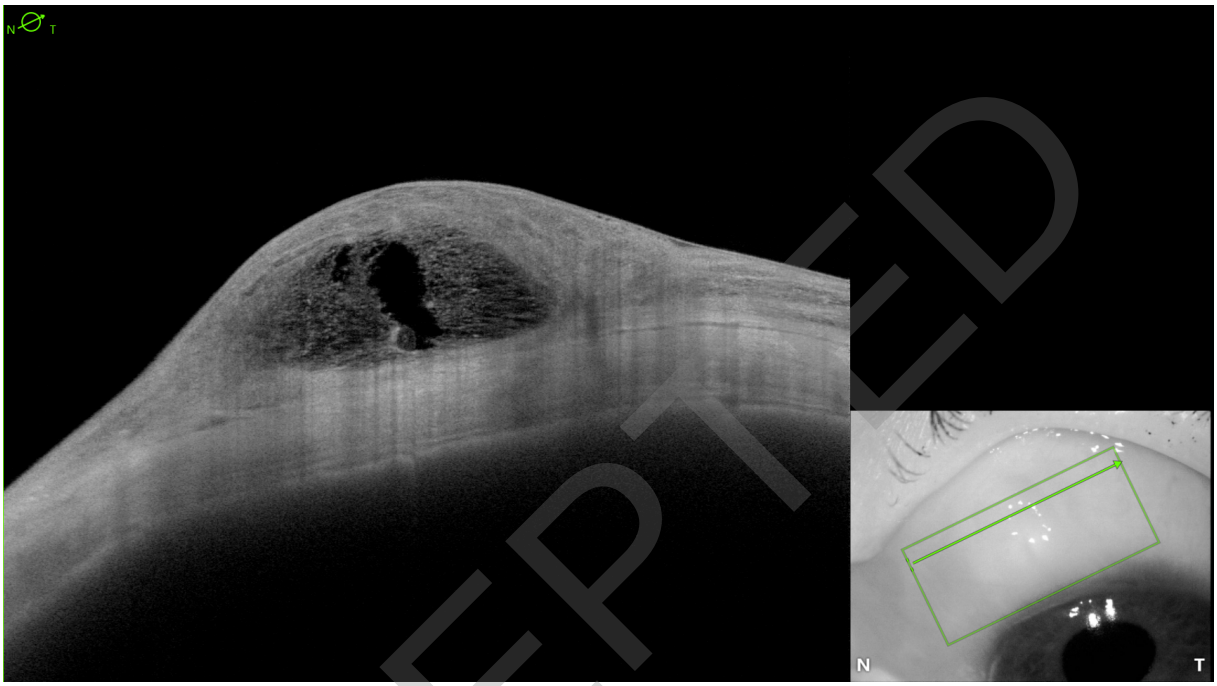

TABLE-1 Inclusion and exclusion criteria.

Abbreviations: MMC: mitomycin C, AS-OCT: Anterior segment optical coherence tomography.

Inclusion Criteria	• Patients undergone implantation of XEN-Gel-Stent with MMC application more than 4 weeks ago • Diagnosed with primary open-angle glaucoma or pseudoexfoliation glaucoma
Exclusion Criteria	• Prior bleb needling or open bleb revision • Prior glaucoma surgery of any kind • Ocular surgery affecting the conjunctiva of any kind (pars plana vitrectomy, strabismus surgery, intravitreal injections, Pterygium surgery … etc.) • Cases in which examination of bleb using AS-OCT was not possible • Low image quality of AS-OCT preventing evaluation of bleb

TABLE-2 Demographic data of included patients

Abbreviations: IOP intraocular pressure.

	Mean± Standard Deviation
Age (years)	65.0±9.3
Number of male participants (%)	20 (42.3%)
Preoperative Intraocular pressure (mmHg)	20.1±4.8
Number of preoperative glaucoma medications	2.9±1.0
Number (%) of patients on	
1 medication	15 (13.5%)
2 medications	19 (17.1%)
3 medications	40 (36%)
4 medications	37 (33.3%)
Number of patients on each medication (%):	
Betablocker	75 (65.8%)
Carbonic anhydrase inhibitor	84 (75.7%)
Alpha 2-agonist	63 (56.8%)
Prostaglandine	95 (85.6%)
Intraocular pressure at 1st post-operative day (mmHg)	9.6±3.4
Post-surgical follow-up time (days)	257.4±249.9
IOP at time of follow-up (mmHg)	15.7±5.1
Number of glaucoma medication at time of examination	0.2±0.6
Change of intraocular pressure compared to baseline (mmHg)	-4.5±6.6
Change of glaucoma medication compared to baseline	-2.7±1.1

TABLE-3 Resulting bleb classification with associated IOP and number of blebs: the conjunctival, tenon and episcleral patterns were added to each other to describe the whole morphology of each bleb and resulted in the classification shown in this table. Most common bleb classification was C2T2ES0 followed by C1T2ES0.

Abbreviations: IOP intraocular pressure, Std. Deviation: standard deviation

Nominal Score System	Mean IOP	Std. Deviation	Number of Blebs
C0T0ES0	21,43	6,554	7
C0T1ES0	17,00	.	1
C0T2ES0	14.5	2.1	2
C0T3ES0	13,20	1,6	5
C1T0ES0	20,43	5,6	7
C1T1ES0	24,00	.	1
C1T1ES1	17,00	.	1
C1T2ES0	16.40	5.9	15
C1T2ES1	14.50	1.9	4
C1T3ES0	16.1	3.3	8
C1T3ES1	13.3	1.1	3
C2T0ES0	23,00	.	1
C2T1ES0	21,50	10.0	4
C2T2ES0	13.0	3.6	34
C2T2ES1	13,00	4,2	2
C2T3ES0	15.2	2.9	16
Total	15.7	5.1	111

TABLE-4 Mean±SD of IOP (intraocular pressure) and number of glaucoma medications in addition to success rates of each pattern in the early post-operative period.

Abbreviations: IOP intraocular pressure, Nr. of Medications: number of medications.

Anatomical Level	Pattern	IOP	Nr. of Medications	Success Rate	N
Conjunctiva	No changes (C0)	20.6±7.9	0.0±0	60%	5
	Epithelial cysts (C1)	19.1±5.4	0.0±0	56%	9
	Subepithelial spaces (C2)	13.0±6.0	0.06±0.2	89%	18
Tenon	No changes (T0)	22.4.3±6.6	0.0±0	43%	7
	Hyperreflective (T1)	19.0±12.1	0.3±0.6	33%	3
	Hyporeflective (T2)	12.8±4.9	0.0±0	94%	16
	Cavernous changes (T3)	15.0±3.7	0.0±0	83%	6
Episcleral Space	Absent episcleral space (ES0)	16.32±7.2	0.4±2.9	71%	28
	Episcleral space visible (ES1)	13.0±2.9	0.0±0	100%	4
All	All	15.9±6.9	0.03±0.2	75%	32

TABLE-5 Mean±SD of IOP and number of glaucoma medications in addition to success rates of each pattern in the late post-operative period.
Abbreviations: IOP intraocular pressure, Nr. of Medications: number of medications.

Anatomical Level	Pattern	IOP	Nr. of Medications	Success Rate	N
Conjunctiva	No changes (C0)	15.9±4.3	0.2±0.4	80%	10
	Epithelial cysts (C1)	16.4±5.0	0.19±0.6	70%	27
	Subepithelial spaces (C2)	15.0±3.7	0.3±0.8	71%	42
Tenon	No changes (T0)	19.9±4.9	0.5±0.7	25%	8
	Hyperreflective (T1)	21.7±3.3	0.25±0.5	25%	4
	Hyporeflective (T2)	14.6±4.1	0.21±0.7	80%	41
	Cavernous changes (T3)	14.9±2.6	0.23±0.6	81%	26
Episcleral Space	Absent episcleral space (ES0)	15.7±4.4	0.26±0.7	70%	71
	Episcleral space visible (ES1)	14.8±1.5	0.0±0	100%	6
All	All	15.6±4.2	0.25±0.7	72%	79